

Joint Trading and Scheduling among Coupled Carbon-Electricity-Heat-Gas Industrial Clusters

Dafeng Zhu, *Member, IEEE*, Bo Yang, *Senior Member, IEEE*, Yu Wu, *Student Member, IEEE*, Haoran Deng, *Student Member, IEEE*, Zhaoyang Dong, *Fellow, IEEE*, Kai Ma, *Member, IEEE* and Xiping Guan, *Fellow, IEEE*

Abstract—This paper presents a carbon-energy coupling management framework for an industrial park, where the carbon flow model accompanying multi-energy flows is adopted to track and suppress carbon emissions on the user side. To deal with the quadratic constraint of gas flows, a bound tightening algorithm for constraints relaxation is adopted. The synergies among the carbon capture, energy storage, power-to-gas further consume renewable energy and reduce carbon emissions. Aiming at carbon emissions disparities and supply-demand imbalances, this paper proposes a carbon trading ladder reward and punishment mechanism and an energy trading and scheduling method based on Lyapunov optimization and matching game to maximize the long-term benefits of each industrial cluster without knowing the prior information of random variables. Case studies show that our proposed trading method can reduce overall costs and carbon emissions while relieving energy pressure, which is important for Environmental, Social and Governance (ESG).

Index Terms—Carbon emission reduction, multi-energy management, carbon capture, industrial park, carbon and multi-energy trading, constraints relaxation, ESG.

I. INTRODUCTION

Nowadays, a large number of industrial clusters (ICs) have settled in the industrial park, which brings huge economic benefits, but forms a concentrated area with high energy consumption and emissions [1]. To reduce emissions and save energy, the industrial park needs to be equipped with green distributed energy systems to improve the energy structure and supply efficiency. Distributed multi-energy systems are built within ICs, which cooperates with gas companies and power grids to satisfy the diverse energy needs of users and achieve energy cascade utilization. The significant role of multi-energy coordination in improving the reliability, economy and cleanliness of energy systems has received extensive attention.

Coal-fired power generation is gradually being replaced by natural gas and renewable power generation [2]. As the increase of gas power generation, the correlation between electricity price and gas price increases. Gas prices affect power generation quotations, unit combinations and optimal scheduling [3], and electricity prices also affect natural gas production and transmission costs. Changes in electricity and

natural gas prices lead to arbitrage behavior, which stimulates electricity and natural gas trading. The power-to-gas (P2G) technology and the increasing share of gas in electricity generation have strengthened the near real-time operational link between gas and electricity systems, which facilitates short-term trades in gas [4].

To increase overall efficiency, unlock synergy potential, and equitably distribute multi-energy generation resources, some countries are moving towards liberalization of energy markets [5]. In Sweden, large-scale boilers and heat pumps are introduced into systems to use excess energy [6]. A project is launched in Germany to tap the potential of heat pumps to increase the utilization of wind energy [7]. The deployment of boilers and heat pumps in Denmark over past decade and the decision to cut taxes in 2013 have created a favorable environment for the electrification of heating [8]. Although the coupled multi-energy market is immature in current practice, the marketing and operational challenges of integrated energy systems have received considerable attention.

Some studies have been conducted on multi-energy trading based on game or auction in industrial and residential parks to improve energy benefit and structure [9]. In [10], an equilibrium model is used to deal with the noncooperative game problem of multi-energy producers, which helps to maximize the energy profit. In [11], a multi-energy game-theoretic bargaining framework is proposed to coordinate multilateral resource and enhance the operational economy and resource utilization. In [12], a multi-energy management framework based on Stackelberg game for heat and electricity trading in an industrial park is constructed to shift the peak load. In [13], auction mechanisms for multi-energy trading are proposed to integrate different energy and supply diverse energy for users. These studies on multi-energy trading effectively achieve complementary sharing among energy sources, but lack consideration of carbon emission reduction among multi-energy ICs with different characteristics, which is indispensable for sustainable development.

With the increasingly serious greenhouse effect caused by the burning of fossil fuels, the issue of emission reduction has attracted widespread attention. In fact, the establishment of a refined and reasonable carbon emission market is of great significance to promote energy marketization and emission reduction [14]. The International Financial Reporting Interpretations Committee describes emission rights as: the government grants participating entities the rights to emit a specific emission level [15]. Since carbon emission right can be purchased and sold to generate income, an active carbon emission market is formed.

Dafeng Zhu, Bo Yang, Yu Wu, Haoran Deng and Xiping Guan are with the Department of Automation, Shanghai Jiao Tong University, Shanghai 200240, China (e-mail: dafeng.zhu@sjtu.edu.cn; bo.yang@sjtu.edu.cn; 5wuuy5@sjtu.edu.cn; denghaoran@sjtu.edu.cn; xpguan@sjtu.edu.cn).

Zhaoyang Dong is with the School of Electrical and Electronic Engineering, Nanyang Technological University, Singapore 639798 (e-mail: zydong@ieee.org).

Kai Ma is with the School of Electrical Engineering, Yanshan University, Qinhuangdao 066004, China (e-mail: kma@ysu.edu.cn).

Chen et al. [16] provide a model of the interrelationships of the gas, electricity and carbon markets and use a relaxed method to deal with the secondary gas flow model. Huang et al. [17] introduce a carbon emission flow model to help multi-energy system planning to achieve low-carbon operation, and propose a generalized circuit theory to deal with the nonlinear model of gas flows. Wei et al. [18] install the wind and photovoltaic (PV) power devices according to system planning to reduce the emissions, and use a linearized model to simplify the secondary function of gas flow between nodes to improve the computability of the planning. Wang et al. [19] establish a low-carbon operation model in a multi-energy system and utilize the carbon capture power plant (CCPP) and P2G technology to greatly reduce the emissions, but ignore the nonlinearity of gas flows. These related studies have realized the economic operation of low-carbon integrated energy systems, but seldom consider the comprehensive impact of multi-energy chain on the environment, the complexity of multi-energy coordination and the nonlinearity of gas flows.

Considering that end users are potential influencers of carbon emissions, so emissions from energy generation should be considered from the demand-side perspective. Kang et al. [20] introduce an emission flow model to clarify the users' emission responsibility. Cheng et al. [21] adopt the carbon emission flow model to allocate emissions from a consumption perspective. Shen et al. [22] apply the emission model to calculate demand-side emissions to evaluate the effect of the low-carbon transformation. Wang et al. [23] adopt a management model to achieve emission reduction by encouraging users to participate in electricity and carbon trading. Although the carbon emission flow models achieve a more accurate calculation of carbon emissions, the above research lacks consideration of the spatiotemporal coupling characteristics of carbon and multi-energy, and the interaction of multi-energy and carbon trading. Carbon and energy coupling means that different sources of energy produce different carbon emissions. For example, renewable energy generation produces no carbon emissions, while coal-fired generation produces high emissions. When ICs trade energy, the carbon emissions in energy is also transferred. This paper takes this into account in carbon and energy trading.

In addition, long-term stochastic optimization problems need to be solved in energy trading. Different from traditional methods like dynamic programming, which requires prior information about the random processes in the system, Lyapunov optimization can give simple online solution to minimize cost and queue fluctuation. Some Lyapunov optimization-based algorithms achieve efficient energy management by transforming the long-term stochastic problem into deterministic subproblems for each time slot [24]. However, it remains difficult to make optimal online scheduling decisions in carbon and energy trading. To achieve effective carbon and energy management among ICs, a multi-energy trading method and a ladder carbon trading mechanism are jointly considered to make optimal scheduling decisions. Compared to existing research, our contributions are summarized.

- 1) A coupled carbon and multi-energy management framework including a CCPP, P2G devices and energy storage

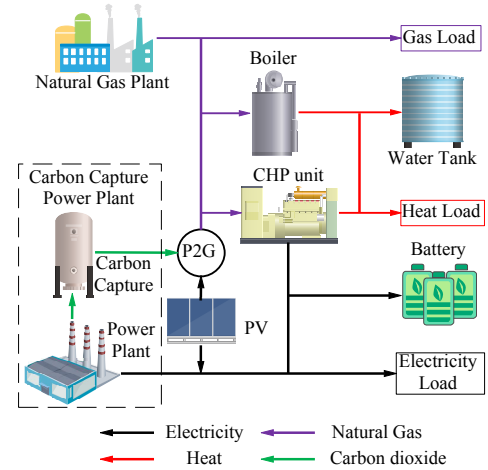


Fig. 1: Multi-energy supply of ICs

for ICs is proposed. The synergies among the CCPP, P2G devices and energy storage further consume renewable energy, reduce carbon emissions, and improve overall benefits. A carbon flow model accompanying multi-energy flows is adopted to track and suppress carbon emissions on the user side.

- 2) To make full use of the differences in carbon emissions and the alternative complementarity of energy, a carbon and energy coordinated trading model is constructed to improve the benefits of the ICs, where the carbon trading ladder reward and punishment mechanism is adopted to improve the willingness to trade. A boundary tightening algorithm is adopted to increase the tightness of the quadratic constraint relaxation of gas flows.
- 3) To alleviate the supply and demand imbalance of individual ICs, a joint trading and scheduling method based on Lyapunov optimization and matching game is proposed, which minimizes the cost of each IC without knowing the prior information of random variables. The matching game provides low-complexity distributed solutions to the energy matching problem between buyers and sellers.

The rest of the work is as follows. The multi-energy devices, carbon emission flow model, energy and carbon trading model among ICs are introduced in Section II. The constraints relaxation of gas flows, joint trading and scheduling method and performance analysis are proposed in Section III. Section IV gives the simulation results. Finally, Section V concludes the paper and presents further research.

II. SYSTEM MODEL

In this paper, a system including an industrial park, a CCPP and a natural gas plant is considered, as shown in Fig. 1. The CCPP consists of a carbon capture device and a power plant, and the amount of carbon capture can be adjusted by changing the power of the carbon capture device. The industrial park consists of ICs and multi-energy devices, which includes CHP units, PV panels, batteries, water tanks, boilers and P2G devices. The industrial park can obtain heat and electricity from CHP units, and store excess energy in water tanks and batteries for the future energy demands.

NOMENCLATURE

- $\pi_{nm}^d(t), \pi_{nm}^s(t)$ Difference and sum of pressures between nodes n and m .
- π_n, π_m Gas pressures at node n and node m .
- $\theta_i(t), \epsilon_i(t)$ Perturbation terms to ensure battery and water tank constraints.
- $B_i(t)$ Electricity of battery i .
- $C_i^{\text{opt}}(t), C_{ir}^{\text{opt}}(t)$ Optimal costs for the original problem and the relaxed problem.
- $C_i(t)$ Total cost of IC i .
- $C_i^c(t)$ Carbon trading cost of IC i .
- $C_i^e(t), D_i^e(t)$ Charge and discharge of battery i .
- $C_i^h(t), D_i^h(t)$ Thermal energy charged and discharged by water tank i .
- $C_i^X(t), R_i^S(t)$ Cost and revenue of IC i for multi-energy trading among ICs.
- C_{nm} Weymouth constant for pipeline nm .
- $E_i(t), p^e(t)$ Electricity and price purchased from the CCP.
- $E_i^{\text{CHP}}(t), H_i^{\text{CHP}}(t), G_i^{\text{CHP}}(t)$ Electricity generation, heat generation and gas consumption of CHP unit i .
- $E_i^d(t), G_i^d(t), H_i^d(t)$ Total electricity, gas and thermal loads of IC i .
- $E_i^o(t), p^o(t)$ Electricity and price sold back to the CCP.
- $E_i^{\text{P2G}}(t), G_i^{\text{P2G}}(t)$ Electricity consumption and gas generation of P2G i .
- $E_i^r(t)$ Electricity generated by PV panel i .
- $F_i(t), Z_i(t)$ Battery and water tank virtual queues for IC i .
- f_{nm} Gas flow from node n to node m .
- $G_i(t), p^g(t)$ Gas and price purchased from the natural gas plant.
- $H_i^b(t), G_i^b(t)$ Heat generation and gas consumption of boiler i .
- i IC, $i \in \{1, 2, \dots, N\}$.
- $p_{ij}^e(t), p_{ij}^g(t)$ Electricity and gas prices that buyer i purchases from seller j .
- $Q_i^a(t), Q_i^d(t)$ Actual and free carbon emissions of IC i .
- $s_{ij}^e(t), s_{ij}^g(t)$ Electricity and gas prices that seller i sells to buyer j .
- t Time slot, $t \in \mathbb{N}$, where \mathbb{N} is the set of natural numbers.
- V_i Tradeoff term between energy cost and queue stability.
- $W_i(t)$ Thermal energy of water tank i .
- $X_i^{\text{eb}}(t), X_i^{\text{es}}(t)$ Electricity purchased and sold by IC i through multi-energy trading among ICs.
- $X_i^{\text{gb}}(t), X_i^{\text{gs}}(t)$ Gas purchased and sold by IC i through multi-energy trading among ICs.

A. Multi-energy Devices

The ICs are equipped with batteries, water tanks, CHP units, boilers, PV panels and P2G devices to supply energy for users according to their energy consumption characteristic. For IC i , $\forall i \in \{1, 2, \dots, N\}$, where N denotes the quantity of ICs in the industrial park, the battery of IC i is denoted as battery i , and the same applies to other devices below. The electricity of the battery i is $B_i(t)$ and the equivalent thermal energy of the hot water tank i is $W_i(t)$, where the time slot $\forall t \in \mathbb{N}$ with \mathbb{N}

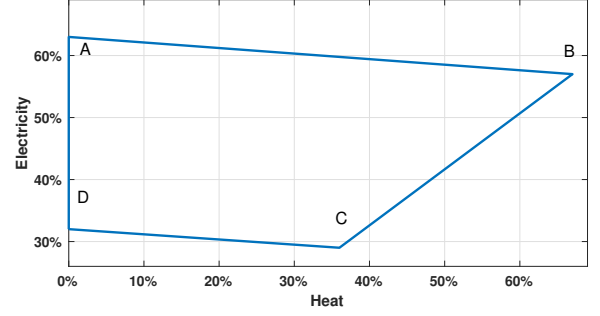


Fig. 2: feasible region for CHP

being the set of natural numbers, and one time slot is a hour. The dynamic models of battery i and water tank i are

$$B_i(t+1) = B_i(t) + C_i^e(t) - D_i^e(t), \forall i, t \quad (1)$$

$$W_i(t+1) = W_i(t) + C_i^h(t) - D_i^h(t), \forall i, t \quad (2)$$

$$B_i^{\min} \leq B_i(t) \leq B_i^{\max}, W_i^{\min} \leq W_i(t) \leq W_i^{\max}, \forall i, t \quad (3)$$

$$0 \leq C_i^e(t) \leq C_i^{e,\max}, 0 \leq D_i^e(t) \leq D_i^{e,\max}, \forall i, t \quad (4)$$

$$0 \leq C_i^h(t) \leq C_i^{h,\max}, 0 \leq D_i^h(t) \leq D_i^{h,\max}, \forall i, t \quad (5)$$

where $C_i^e(t)$ and $D_i^e(t)$ denote the charging and discharging amount of battery i . $C_i^h(t)$ and $D_i^h(t)$ are the thermal energy charging and discharging amount of hot water tank i .

The CHP unit, as a co-generation unit, can generate both heat and electricity by consuming natural gas $G_i^{\text{CHP}}(t)$. However, the generation of heat $H_i^{\text{CHP}}(t)$ and electricity $E_i^{\text{CHP}}(t)$ cannot be separately considered. The co-generation is coupled and interdependent. The generation constraints of the CHP unit are operated in a feasible region which is depicted in Fig. 2 [25]. The feasible operating region is bounded by curve ABCD. A, B, C and D represent four marginal points of the feasible region for the CHP unit. In order to describe the feasible region of CHP unit i , we have the following inequality constraints

$$E_i^{\text{CHP}}(t) - E_i^{\text{CHP},A} - \frac{E_i^{\text{CHP},A} - E_i^{\text{CHP},B}}{H_i^{\text{CHP},A} - H_i^{\text{CHP},B}} (H_i^{\text{CHP}}(t) - H_i^{\text{CHP},A}) \leq 0, \forall i, t \quad (6)$$

$$E_i^{\text{CHP}}(t) - E_i^{\text{CHP},B} - \frac{E_i^{\text{CHP},B} - E_i^{\text{CHP},C}}{H_i^{\text{CHP},B} - H_i^{\text{CHP},C}} (H_i^{\text{CHP}}(t) - H_i^{\text{CHP},B}) \geq 0, \forall i, t \quad (7)$$

$$E_i^{\text{CHP}}(t) - E_i^{\text{CHP},C} - \frac{E_i^{\text{CHP},C} - E_i^{\text{CHP},D}}{H_i^{\text{CHP},C} - H_i^{\text{CHP},D}} (H_i^{\text{CHP}}(t) - H_i^{\text{CHP},C}) \geq 0, \forall i, t \quad (8)$$

$$0 \leq H_i^{\text{CHP}}(t) \leq H_i^{\text{CHP},B}, \forall i, t \quad (9)$$

$$0 \leq E_i^{\text{CHP}}(t) \leq E_i^{\text{CHP},A}, \forall i, t \quad (10)$$

Eq. (6) denotes the area under the curve AB. Eq. (7) and Eq. (8) denote the area above the curve BC and CD respectively.

The boiler i generates heat $H_i^b(t)$ by consuming natural gas $G_i^b(t)$, which is

$$H_i^b(t) = \eta_i^{\text{bg}} G_i^b(t), 0 \leq H_i^b(t) \leq H_i^{b,\max}, \forall i, t \quad (11)$$

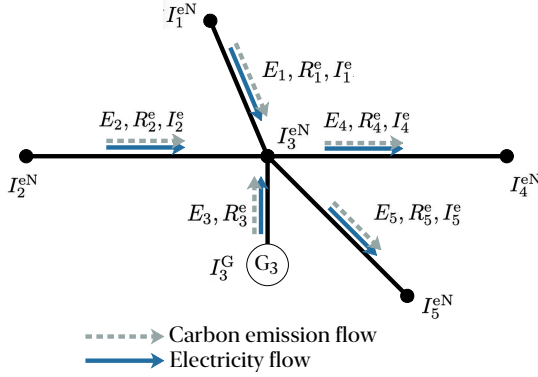


Fig. 3: Carbon emission accompanying the electricity flow

where η_{ibg} denotes the efficiency of boiler i to generate heat.

The amount of electricity generated by PV panel i is $E_i^r(t)$. The amount of electricity consumed and gas generated by P2G device i are $E_i^{p2g}(t)$ and $G_i^{p2g}(t)$. The models of PV panel i and P2G i are denoted as

$$0 \leq E_i^r(t) \leq E_i^{r,\max}, \forall i, t \quad (12)$$

$$G_i^{p2g}(t) = \eta_i^{p2g} E_i^{p2g}(t), 0 \leq G_i^{p2g}(t) \leq G_i^{p2g,\max}, \forall i, t \quad (13)$$

where η_i^{p2g} is the efficiency of P2G i .

B. Carbon Emission Flow Model

In order to obtain the emissions corresponding to energy consumption on the consumer side, and track the carbon footprints of different energy forms in the multi-energy system of the industrial park, a carbon flow model accompanying multi-energy flows is introduced to calculate the emissions of ICs [26].

1) *Carbon Emission Accompanying Electricity Flow*: According to the basic principles of [26], the carbon emission intensity of a node is determined by the emissions flowing into the node, which is equal to the carbon emission intensity of the outflow line of the node. Taking node 3 in electricity network as an example in Fig. 3, the carbon emission intensity I_3^{eN} of node 3 equals the carbon intensity of lines 4 and 5, which is denoted by

$$I_3^{eN} = \frac{E_1 I_1^e + E_2 I_2^e + E_3^G I_3^G}{E_1 + E_2 + E_3^G} = \frac{R_1^e + R_2^e + R_3^G}{E_1 + E_2 + E_3^G} = I_4^e = I_5^e \quad (14)$$

where E_1 , E_2 and E_3^G denote the electricity flows of lines 1, 2 and generator 3. I_1^e , I_2^e and I_3^G denote the carbon emission intensities of lines 1, 2 and generator 3. R_1^e , R_2^e and R_3^G denote the carbon emissions of lines 1, 2 and generator 3.

According to the carbon intensity at node 3, the carbon intensity at node n is deduced by

$$I_n^{eN} = \frac{\sum_{m \in M} E_m I_m^e + E_n^G I_n^G}{\sum_{m \in M} E_m + E_n^G} = \frac{\sum_{m \in M} R_m^e + R_n^G}{\sum_{m \in M} E_m + E_n^G}, \forall n \quad (15)$$

where M is the line set of emissions flowing into node n .

2) *Carbon Emission Accompanying Gas Flow*: In the natural gas pipeline, compressors are equipped to compensate the pressure losses caused by resistance to ensure the reliable gas delivery. The carbon emission R_c of compressor c is denoted as

$$R_c = I_c^{eN} E_c^o, \forall c \quad (16)$$

where I_c^{eN} and E_c^o denote the nodal carbon intensity and electricity consumption of compressor c . The emissions R_p^g of gas pipeline p are the sum of the emissions from the compressor and the emissions accompanying the gas flow, which is denoted as

$$R_p^g = I_p^g f_p^g B + R_c, \forall p \quad (17)$$

where I_p^g denotes the carbon intensity of gas pipeline p ; f_p^g denote the gas flow of pipeline p ; B is the calorific value of gas, which is 10 kWh/m³. The nodal carbon intensity I_n^{gN} of gas, which is similar as the one of electricity, is denoted as

$$I_n^{gN} = \frac{\sum_p R_p^g + f_w I_w^{gC} B}{(\sum_p f_p^g + f_w) B}, \forall n, w \quad (18)$$

where I_w^{gC} denotes the carbon emission per unit of gas combustion, which is 0.2 kgCO₂/kWh. f_w denotes the gas flow of gas source w in node n . The gas f_{nm} flowing from node n to node m in the pipeline $\forall nm \in \Omega_p$ with Ω_p being the set of gas pipelines is denoted as

$$f_{nm}^2 = C_{nm}^2 (\pi_n^2 - \pi_m^2), \forall nm \quad (19)$$

$$\pi^{\min} \leq \pi \leq \pi^{\max} \quad (20)$$

$$\rho^{\min} \leq \frac{\pi_n}{\pi_m} \leq \rho^{\max}, \forall nm \quad (21)$$

where C_{nm} denote the Weymouth constant for pipeline nm . π_n and π_m are the gas pressures at nodes n and m .

The carbon intensity I_n^{hN} of heat load at node n is similar to the carbon intensity of electricity load at node n .

C. Carbon Trading

Each IC i is allocated free carbon emissions $Q_i^d(t)$ based on industry benchmarks.

The actual emissions are related to the energy load and its carbon intensity, where the CCPP can capture CO₂ to reduce the actual emission of ICs. The actual emissions of IC i are

$$Q_i^a(t) = \sum_{n \in L_i^e} I_n^{eN}(t) E_n^d(t) + \sum_{n \in L_i^g} I_n^{gN}(t) G_n^d(t) B + \sum_{n \in L_i^h} I_n^{hN}(t) H_n^d(t) - \eta^{cc} b^{cc} E_i^{cc}(t), \forall n, t \quad (22)$$

where L_i^e , L_i^g and L_i^h are the electricity, gas and thermal load node sets of IC i . $E_n^d(t)$, $G_n^d(t)$ and $H_n^d(t)$ are electricity, gas and heat loads of node n . η^{cc} , b^{cc} and $E_i^{cc}(t)$ denote the carbon capture efficiency, unit carbon emissions and electricity generation of the CCPP for IC i .

To encourage ICs to reduce emissions and use green energy, the ladder reward and punishment carbon trading mechanism is introduced. The more the actual carbon emissions exceed the allocated carbon emissions, the faster trading costs increase.

The carbon trading cost of IC i , $\forall i$, can be denoted in (23), where the time slot t is removed for simplicity.

$$C_i^c = \begin{cases} -p^c(1+k\beta)(Q_i^d - Q_i^a - kl) - (k + \frac{(k-1)k\beta}{2})p^cl, & \text{if } Q_i^d - (k+1)l < Q_i^a \leq Q_i^d - kl \\ -p^c(1+\beta)(Q_i^d - Q_i^a - l) - p^cl, & \text{if } Q_i^d - 2l < Q_i^a \leq Q_i^d - l \\ -p^c(Q_i^d - Q_i^a), \text{if } Q_i^d - l < Q_i^a \leq Q_i^d \\ p^c(Q_i^a - Q_i^d), \text{if } Q_i^d < Q_i^a \leq Q_i^d + l \\ p^c(1+\alpha)(Q_i^a - Q_i^d - l) + p^cl, & \text{if } Q_i^d + l < Q_i^a \leq Q_i^d + 2l \\ p^c(1+k\alpha)(Q_i^a - Q_i^d - kl) + (k + \frac{(k-1)k\alpha}{2})p^cl, & \text{if } Q_i^d + kl < Q_i^a \leq Q_i^d + (k+1)l \end{cases} \quad (23)$$

where p^c denotes the unit price of carbon emission allowances. α and β are the punishment and reward factors, respectively. l denotes the length of emission interval, where there are $2K$ intervals, $k = 1, 2, 3, \dots, K$. When the difference between the carbon emission quota and the actual carbon emissions does not exceed l , the price of carbon trading is p^c . Thereafter, whenever the difference between carbon emission quota and actual carbon emissions exceeds an interval length l , the carbon trading price for the excess part will increase by αp^c . For example, when the actual carbon emission of IC i exceeds its carbon emission quota by $1.4l$, the price of trading l carbon emission right is p^c , and the price of carbon right for the excess $0.4l$ is $(1+\alpha)p^c$.

D. Multi-Energy Trading

To satisfy multi-energy demand, ICs in the industrial park can trade gas and electricity with each other. The deal energy price and quantity are calculated by the multi-energy trading and scheduling method, which is elaborated in Section III.

According to the deal energy price and quantity, the cost $C_i^X(t)$ and revenue $R_i^S(t)$ of IC i are

$$C_i^X(t) = \sum_j p_{ij}^e(t) X_{ij}^{eb}(t) + \sum_j p_{ij}^g(t) X_{ij}^{gb}(t), \forall i, t \quad (24)$$

$$R_i^S(t) = \sum_j s_{ij}^e(t) X_{ij}^{es}(t) + \sum_j s_{ij}^g(t) X_{ij}^{gs}(t), \forall i, t \quad (25)$$

where $p_{ij}^e(t)$ and $p_{ij}^g(t)$ are the electricity and gas prices that buyer i purchases from seller j . $X_{ij}^{eb}(t)$ and $X_{ij}^{gb}(t)$ denote the quantities of energy purchased by buyer i from seller j . $s_{ij}^e(t)$ and $s_{ij}^g(t)$ denote the energy prices sold by seller i to buyer j . $X_{ij}^{es}(t)$ and $X_{ij}^{gs}(t)$ are the quantities of energy sold by seller i to buyer j . This paper mainly considers the influence of node pressure on gas flow in natural gas trading. $\forall ij \in \Omega_c$ with Ω_c being the set of ICs that trade energy with each other. The gas purchased by IC i from the node n of IC j is delivered to the node m of IC i through the pipeline nm

$$X_{ij}^{gb}(t) = f_{nm}(t), \forall ij, nm, t \quad (26)$$

When the energy in the trading market among ICs is insufficient, IC i will purchase electricity $E_i(t)$ and gas $G_i(t)$ from the CCPP and natural gas plant. When the renewable

energy generation is surplus, IC i will sell electricity $E_i^o(t)$ to the CCPP. The constraints on energy trading with plants are

$$\begin{aligned} 0 \leq E_i(t) \leq E_i^{\max}, 0 \leq G_i(t) \leq G_i^{\max}, \\ 0 \leq E_i^o(t) \leq E_i^{o,\max}, \forall i, t \end{aligned} \quad (27)$$

E. Energy Demand

The total electricity $E_i^d(t)$, gas $G_i^d(t)$ and heat $H_i^d(t)$ demands of the users in IC i are satisfied by multi-energy devices and utility companies.

$$\begin{aligned} E_i^d(t) = E_i(t) - E_i^o(t) + X_i^{eb}(t) - X_i^{es}(t) + D_i^e(t) \\ - C_i^e(t) + E_i^{\text{CHP}}(t) - E_i^{\text{p2g}}(t) + E_i^f(t), \forall i, t \end{aligned} \quad (28)$$

$$\begin{aligned} G_i^d(t) = G_i(t) - G_i^{\text{CHP}}(t) - G_i^b(t) + X_i^{gb}(t) - X_i^{gs}(t) \\ + G_i^{\text{p2g}}(t), \forall i, t \end{aligned} \quad (29)$$

$$H_i^d(t) = H_i^{\text{CHP}}(t) + H_i^b(t) + D_i^h(t) - C_i^h(t), \forall i, t \quad (30)$$

$$X_i^{eb}(t) = \sum_j X_{ij}^{eb}(t), X_i^{es}(t) = \sum_j X_{ij}^{es}(t), \forall i, t \quad (31)$$

$$X_i^{gb}(t) = \sum_j X_{ij}^{gb}(t), X_i^{gs}(t) = \sum_j X_{ij}^{gs}(t), \forall i, t \quad (32)$$

Gas is not used directly, but converted into heat and electricity to satisfy users' demands, so $G_i^d(t)$ is 0.

F. Cost Function

The total cost of IC i consists of the trading cost and revenue

$$\begin{aligned} C_i(t) = C_i^c(t) + E_i(t)p^e(t) - E_i^o(t)p^o(t) \\ + [G_i^{\text{CHP}}(t) + G_i^b(t)]p^g(t) + C_i^X(t) - R_i^S(t), \forall i, t \end{aligned} \quad (33)$$

where $p^e(t)$ denotes the electricity price of the CCPP and $p^g(t)$ denotes the natural gas price. $p^o(t)$ denotes the electricity price sold back to the CCPP.

The aim of IC i is to minimize the total cost with the time-varying characteristics of energy supply and demand

$$\min_{M_i(t)} \lim_{T \rightarrow \infty} \frac{1}{T} \sum_{t=0}^{T-1} \mathbb{E}\{C_i(t)\}, \forall i \quad (34)$$

s.t. (1) – (30)

where $M_i(t) = \{D_i^e(t), C_i^e(t), D_i^h(t), C_i^h(t), E_i^o(t), E_i(t), E_i^{\text{p2g}}(t), G_i^{\text{CHP}}(t), G_i^b(t), X_i^{eb}(t), X_i^{gb}(t), X_i^{es}(t), X_i^{gs}(t)\}$, $\forall i, t$ denotes the set of optimization variables.

III. SOLUTION METHOD

Different from traditional methods like dynamic programming, which requires priori information of the random processes in the system and has high computational complexity, Lyapunov optimization can give simple online solutions according to the current information about the system state. The performance of the Lyapunov optimization-based algorithm can be arbitrarily close to the optimal performance [27]. Fundamental assumptions about future information unavailability make offline methods impractical for systems with a high

degree of uncertainty, and dynamic programming is unsuitable for multiple networked energy storage systems [28].

Firstly, Lyapunov optimization is introduced to convert the original problem into a weighted cost minimization problem for each slot, which can make control decisions to weigh the overall energy cost and energy storage stability. Then, a bound tightening algorithm is adopted to handle the relaxation problem of the quadratic constraint on gas transmission among ICs. Finally, the energy trading among ICs is determined by matching game.

A. Lyapunov optimization

In order to handle the coupling constraints of electricity and heat charging/discharging, the time-average constraints of the relaxed problem are used to replace the coupling constraints (1) and (2) of the original problem

$$\begin{aligned} \lim_{T \rightarrow \infty} \frac{1}{T} \sum_{t=0}^{T-1} \mathbb{E}\{C_i^e(t)\} &= \lim_{T \rightarrow \infty} \frac{1}{T} \sum_{t=0}^{T-1} \mathbb{E}\{D_i^e(t)\}, \forall i \\ \lim_{T \rightarrow \infty} \frac{1}{T} \sum_{t=0}^{T-1} \mathbb{E}\{C_i^h(t)\} &= \lim_{T \rightarrow \infty} \frac{1}{T} \sum_{t=0}^{T-1} \mathbb{E}\{D_i^h(t)\}, \forall i \end{aligned} \quad (35)$$

C_i^{opt} denotes the optimal cost of the original problem and C_{ir}^{opt} denotes the optimal cost of the relaxed problem. Since the relaxed problem has fewer constraints than the original problem, $C_{ir}^{\text{opt}} \leq C_i^{\text{opt}}$ holds.

The stationary and randomized policy Π is introduced to obtain the optimal solution of the relaxed problem

$$\mathbb{E}\{C_i^{\Pi}(t)\} = C_{ir}^{\text{opt}}, \forall i, t \quad (36)$$

subject to:

$$\begin{aligned} C_i^{e,\Pi}(t) &= D_i^{e,\Pi}(t), \forall i, t \\ C_i^{h,\Pi}(t) &= D_i^{h,\Pi}(t), \forall i, t \end{aligned} \quad (37)$$

and (4) - (30).

The policy Π can be ensured by the Caratheodory theory, similar to [29]. Clearly, solutions to the relaxed problem are feasible to the original problem only if they satisfy the constraint (3). To achieve the goal, virtual energy storage queues $F_i(t)$ and $Z_i(t)$ are constructed as $F_i(t) = B_i(t) - \theta_i$, $Z_i(t) = W_i(t) - \varepsilon_i$, $\forall i, t$. θ_i and ε_i are utilized to ensure $B_i(t)$ and $W_i(t)$ satisfy the upper limits [30].

The Lyapunov function and Lyapunov drift are

$$Y_i(t) = \frac{1}{2}F_i(t)^2 + \frac{1}{2}Z_i(t)^2, \forall i, t \quad (38)$$

$$\Delta_i(t) = \mathbb{E}\{Y_i(t+1) - Y_i(t) | B_i(t), W_i(t)\}, \forall i, t \quad (39)$$

where the expectation is with respect to the stochastic process of the system, given $B_i(t)$ and $W_i(t)$. According to the virtual queue $F_i(t)$ and $Z_i(t)$, the Lyapunov drift has the upper bound

$$\begin{aligned} \Delta_i(t) &\leq A_i + \mathbb{E}\{F_i(t)(C_i^e(t) - D_i^e(t)) \\ &\quad + Z_i(t)(C_i^h(t) - D_i^h(t))\}, \forall i, t \\ A_i &= \frac{1}{2}[\max((C_i^{e,\max})^2, (D_i^{e,\max})^2) \\ &\quad + \max((C_i^{h,\max})^2, (D_i^{h,\max})^2)] \end{aligned} \quad (40)$$

The proof of this step can refer to [30].

To minimize overall cost of the IC while ensuring energy storage stability, V_i is used to control the tradeoff between energy cost and queue stability. The corresponding drift-plus-penalty term is

$$\begin{aligned} &\Delta_i(t) + V_i \mathbb{E}\{C_i(t)\} \\ &\leq A_i + \mathbb{E}\{F_i(t)(C_i^e(t) - D_i^e(t)) + Z_i(t)(C_i^h(t) - D_i^h(t)) \\ &\quad + V_i(C_i^e(t) + E_i(t)p^e(t) - E_i^o(t)p^o(t) + C_i^X(t) - R_i^S(t) \\ &\quad + (G_i^{\text{CHP}}(t) + G_i^b(t))p^g(t)\}, \forall i, t \end{aligned} \quad (41)$$

The original optimization problem (34) is converted to minimize $\Gamma_i(t)$

$$\begin{aligned} &\min_{M_i(t)} \Gamma_i(t) \\ &= \min_{M_i(t)} F_i(t)(C_i^e(t) - D_i^e(t)) + Z_i(t)(C_i^h(t) - D_i^h(t)) \\ &\quad + V_i(C_i^e(t) + E_i(t)p^e(t) - E_i^o(t)p^o(t) + C_i^X(t) - R_i^S(t) \\ &\quad + (G_i^{\text{CHP}}(t) + G_i^b(t))p^g(t)), \forall i, t \\ &\text{s.t. (4) - (30)} \end{aligned} \quad (42)$$

B. Constraints Relaxation of Gas flows

Owing to the quadratic constraint (19) on gas transmission among ICs, the system model is nonlinear. To deal with the nonlinear problem, the quadratic constraint (19) is replaced by

$$\frac{f_{nm}^2(t)}{C_{nm}^2} \geq \pi_n^2(t) - \pi_m^2(t), \forall nm, t \quad (43)$$

$$\frac{f_{nm}^2(t)}{C_{nm}^2} \leq \pi_n^2(t) - \pi_m^2(t), \forall nm, t \quad (44)$$

After relaxing (43) and replacing (19) with (44), the trading and scheduling optimization problem can be solved with second-order cone programming. However, the relaxed constraints may lead to serious violations of (19). Thus, a relaxation method based on quadratic convex relaxation [31] is introduced to guarantee the approximation of the constraint (19). To avoid the extra computation and less tight relaxation caused by individually approximating $\pi_n^2(t)$ and $\pi_m^2(t)$, the pressure difference $\pi_{nm}^d(t)$ and the pressure sum $\pi_{nm}^s(t)$ between nodes n and m are introduced

$$\pi_{nm}^d(t) = \pi_n(t) - \pi_m(t), \forall nm, t \quad (45)$$

$$\pi_{nm}^s(t) = \pi_n(t) + \pi_m(t), \forall nm, t \quad (46)$$

The relaxation of (43) is denoted as

$$\frac{F_{nm}(t)}{C_{nm}^2} \geq \Pi_{nm}(t), \forall nm, t \quad (47)$$

$$F_{nm}(t) \geq f_{nm}^2(t), \forall nm, t \quad (48)$$

$$\begin{aligned} F_{nm}(t) &\leq (f_{nm}^{\max}(t) + f_{nm}^{\min}(t))f_{nm}(t) - f_{nm}^{\max}(t)f_{nm}^{\min}(t), \\ &\quad \forall nm, t \\ \Pi_{nm}(t) &\geq \pi_{nm}^{d,\min}(t)(\pi_{nm}^s(t) - \pi_{nm}^{s,\min}(t)) + \pi_{nm}^{s,\min}(t)\pi_{nm}^d(t), \\ &\quad \forall nm, t \end{aligned} \quad (49)$$

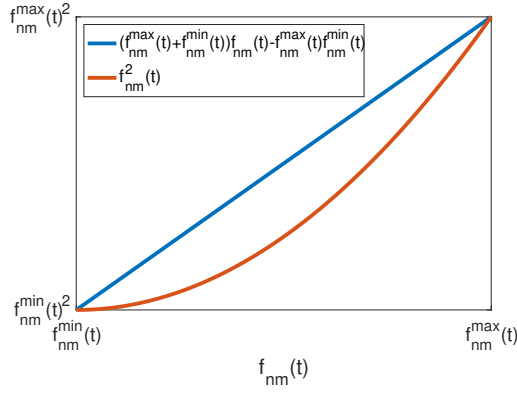


Fig. 4: Approximation of $f_{nm}^2(t)$ according to (48) and (49).

$$\Pi_{nm}(t) \geq \pi_{nm}^{d,\max}(t)(\pi_{nm}^s(t) - \pi_{nm}^{s,\max}(t)) + \pi_{nm}^{s,\max}(t)\pi_{nm}^d(t), \quad \forall nm, t \quad (51)$$

$$\Pi_{nm}(t) \leq \pi_{nm}^{d,\min}(t)(\pi_{nm}^s(t) - \pi_{nm}^{s,\max}(t)) + \pi_{nm}^{s,\max}(t)\pi_{nm}^d(t), \quad \forall nm, t \quad (52)$$

$$\Pi_{nm}(t) \leq \pi_{nm}^{d,\max}(t)(\pi_{nm}^s(t) - \pi_{nm}^{s,\min}(t)) + \pi_{nm}^{s,\min}(t)\pi_{nm}^d(t), \quad \forall nm, t \quad (53)$$

where $F_{nm}(t)$ and $\Pi_{nm}(t)$ denote approximations of $f_{nm}^2(t)$ and $\pi_n^d(t) - \pi_m^d(t)$ to achieve the replacement of (43) with (47). Fig. 4 shows that convex boundary constraints (48)-(49) of $f_{nm}^2(t)$ impose the bounds on $F_{nm}(t)$. Likewise, convex boundary constraints (50)-(53) of $\pi_n^d(t) - \pi_m^d(t)$ (i.e., $\pi_{nm}^d(t)\pi_{nm}^s(t)$) impose similar bounds on $\Pi_{nm}(t)$. The optimization problem (42) is converted to the relaxed problem

$$\min_{M_i(t)} \Gamma_i(t), \forall i, t \quad (54)$$

$$\text{s.t. (4) - (18), (20) - (30), (44) - (53)}$$

Fig. 4 shows that the approximate effect of the constraints (48)-(49) depends on the values $f_{nm}^{\min}(t)$, $f_{nm}^{\max}(t)$. For instance, the maximum deviation between $f_{nm}^2(t)$ and $(f_{nm}^{\max}(t) + f_{nm}^{\min}(t))f_{nm}(t) - f_{nm}^{\max}(t)f_{nm}^{\min}(t)$ is $[(f_{nm}^{\max}(t) - f_{nm}^{\min}(t))/2]^2$. Similarly, the approximate effect of the constraints (50)-(53) depends on the values $\pi_{nm}^{d,\min}(t)$, $\pi_{nm}^{d,\max}(t)$, $\pi_{nm}^{s,\min}(t)$ and $\pi_{nm}^{s,\max}(t)$.

Algorithm 1 : Bound Tightening Algorithm

- 1: **Initialize:** $f_{nm}^{\min}(t)$, $f_{nm}^{\max}(t)$, $\pi_{nm}^{d,\min}(t)$, $\pi_{nm}^{d,\max}(t)$, $\pi_{nm}^{s,\min}(t)$, $\pi_{nm}^{s,\max}(t)$.
- 2: **for** $o = 1, 2, \dots, O$ **do**
- 3: Solve the relaxed problem to obtain $f_{nm,o}(t)$, $\pi_{nm,o}^d(t)$ and $\pi_{nm,o}^s(t)$.
- 4: $f_{nm}^{\min}(t) \leftarrow (1 - \sigma_o)f_{nm,o}(t)$, $f_{nm}^{\max}(t) \leftarrow (1 + \sigma_o)f_{nm,o}(t)$.
- 5: $\pi_{nm}^{d,\min}(t) \leftarrow (1 - \sigma_o)\pi_{nm,o}^d(t)$, $\pi_{nm}^{d,\max}(t) \leftarrow (1 + \sigma_o)\pi_{nm,o}^d(t)$.
- 6: $\pi_{nm}^{s,\min}(t) \leftarrow (1 - \sigma_o)\pi_{nm,o}^s(t)$, $\pi_{nm}^{s,\max}(t) \leftarrow (1 + \sigma_o)\pi_{nm,o}^s(t)$.
- 7: **Until** $|\pi_n^d(t) - \pi_m^d(t) - f_{nm}^2(t)/C_{nm}^2| \leq \delta\pi_n^d(t)$.
- 8: **end for**

Therefore, a bound tightening algorithm is presented to enhance the tightness of the proposed relaxation. Algorithm 1 shows the process of the bound tightening algorithm, where the variable σ_o is gradually reduced to ensure that the upper and lower bounds converge within the tight range where the optimal solution lies, and δ is the convergence threshold.

C. Matching Game

Due to energy supply and demand imbalance in individual ICs, energy needs to be shared among ICs. First, the submitted selling price or purchase price of IC i is determined in energy trading according to [30]. Then, the amount of energy sold by sellers and purchased by buyers are obtained by solving the problem (54). The two sides of the transaction can be determined by the matching game.

The matching theory based on the preference and information of ICs provides low-complexity distributed solutions to the energy matching problem between sellers and buyers. Thus, a many-to-many matching game model is introduced, where a seller can sell energy to several buyers and a buyer can purchase energy from several sellers. I and J respectively denote the set of buyers and sellers in the trading market. A matching game μ is defined as a mapping from set $I \cup J$ into all subsets of set $I \cup J$, where 1) $\forall i \in I$, $\mu(i) \in J$; 2) $\forall j \in J$, $\mu(j) \in I$; 3) if and only if $\mu(i) = j$, $\mu(j) = i$.

For any buyer $i \in I$, it will choose seller j that can maximize its energy trading revenue. The revenue of buyer i is denoted as $U_i(j) = -C_i^X(t) = -\sum_j p_{ij}^e(t)X_{ij}^{eb}(t) - \sum_j p_{ij}^g(t)X_{ij}^{gb}(t)$, $\forall i, t$. Similarly, the revenue of seller j is denoted as $U_j(i) = \sum_i s_{ij}^e(t)X_{ij}^{es}(t) + \sum_i s_{ij}^g(t)X_{ij}^{gs}(t)$, $\forall j, t$. The deal energy price is the average of matching bid and ask quotes.

A preference relation \succ is introduced to rank the preference list of buyers and sellers. \succ_i of buyer i is used to rank sellers over the set of J , where $j \succ_i j' \Leftrightarrow U_i(j) > U_i(j')$. Similarly, $i \succ_j i' \Leftrightarrow U_j(i) > U_j(i')$.

With the preference relations and the utility functions of buyers and sellers, the energy trading problem between buyers and sellers is solved by the matching game based energy trading algorithm, as shown in Algorithm 2. The algorithm 2 can converge to a stable matching [32], i.e., there does not exist a buyer $i' \in I$ such that $i' \succ_j \mu(j)$, $\forall j$. After determining the energy trading among ICs, the optimal solution set $M_i^*(t)$ of each IC can be obtained by solving the problem (54). The whole procedure of the proposed method is shown in Algorithm 3.

Algorithm 2 : Matching Game Based Trading Algorithm

- 1: **while** unstable matching **do**
- 2: Update each buyer's preference list about sellers according to $U_i(j)$, and send its intention to its most preferred seller.
- 3: Update each seller's preference list about the intentional and matched buyers according to $U_j(i)$.
- 4: **repeat:**
- 5: Randomly choose a seller j to sell its energy to its most preferred buyers. If the energy of j was matched by other buyer i' , remove the energy of j from the matching energy of i' .
- 6: **until** The seller sells all energy or all preferred buyers are matched.
- 7: When a buyer buys the energy it needs, remove it from I .
- 8: When a seller sells all energy, remove it from J .
- 9: **end while**

D. Performance Analysis

In the above methods, we consider the battery and water tank of IC i as follows

Algorithm 3 : The Procedure of the Proposed Method

- 1: **Initialize:** $B_i(t), W_i(t)$.
 - 2: **for** IC i **do**
 - 3: Calculate the submitted selling and purchase prices of IC i , and calculate $X_i^{eb}(t), X_i^{gb}(t), X_i^{es}(t)$ and $X_i^{gs}(t)$ by (54) based on Lyapunov optimization and the bound tightening algorithm.
 - 4: Calculate $p_{ij}^e(t), s_{ij}^e(t), p_{ij}^g(t), s_{ij}^g(t), X_{ij}^{eb}(t), X_{ij}^{gb}(t), X_{ij}^{es}(t)$ and $X_{ij}^{gs}(t)$ by the matching game.
 - 5: Calculate $M_i(t)$ using (54).
 - 6: **end for**
 - 7: Calculate $B_i(t+1)$ and $W_i(t+1)$ by (1) - (2).
-

Lemma 1. When θ_i, ϵ_i and V_i are set as

$$\begin{aligned}
 \theta_i &= V_i p^{e,\max} + D_i^{e,\max} \\
 \epsilon_i &= \frac{V_i p^{g,\max}}{\eta_i^{\text{bg}}} + D_i^{\text{h},\max} \\
 V_i^{\max} &= \min \left\{ \frac{B_i^{\max} - C_i^{e,\max} - D_i^{e,\max}}{p^{e,\max}}, \right. \\
 &\quad \left. \frac{\eta_i^{\text{bg}} (W_i^{\max} - C_i^{\text{h},\max} - D_i^{\text{h},\max})}{p^{g,\max}} \right\}, \quad (55) \\
 0 &\leq V_i \leq V_i^{\max}, \forall i
 \end{aligned}$$

the energy storage capacity constraints of IC i are always satisfied.

Proof. The mathematical induction is adopted to prove that the capacity constraints of $B_i(t)$ are always satisfied, $\forall i$. Clearly, the proposition holds at time slot 0. Then, the proposition is assumed to hold at time slot t , we prove that the proposition holds at time slot $t+1$ through the following four situations.

- 1) Situation 1: $B_i(t) > \theta_i$. In this situation, $F_i(t) = B_i(t) - \theta_i > 0$. According to the optimization problem (54), $C_i^e(t) = 0$. Thus, $B_i(t+1) \leq B_i(t) \leq B_i^{\max}$.
- 2) Situation 2: $B_i(t) \leq \theta_i$. In this situation, since $C_i^e(t) \leq C_i^{e,\max}$ and $\theta_i = V_i p^{e,\max} + D_i^{e,\max} \leq B_i^{\max} - C_i^{e,\max}$, $B_i(t+1) \leq B_i(t) + C_i^{e,\max} < \theta_i + C_i^{e,\max} \leq B_i^{\max}$.
- 3) Situation 3: $B_i(t) < D_i^{e,\max}$. In this situation, $F_i(t) = B_i(t) - \theta_i < D_i^{e,\max} - \theta_i = -V_i p^{e,\max}$. From (28), we can get $C_i^e(t) - D_i^e(t) = E_i(t) - E_i^o(t) + X_i^{eb}(t) - X_i^{es}(t) + E_i^{\text{CHP}}(t) - E_i^{\text{p2g}}(t) + E_i^r(t) - E_i^d(t)$. According to (54), we can get

$$\begin{aligned}
 &\min_{M_i(t)} \Gamma_i(t) \\
 &= \min_{M_i(t)} (F_i(t) + V_i p^e(t)) E_i(t) + F_i(t) (-E_i^o(t) \\
 &\quad + X_i^{eb}(t) - X_i^{es}(t) + E_i^{\text{CHP}}(t) - E_i^{\text{p2g}}(t) \\
 &\quad + E_i^r(t) - E_i^d(t)) + Z_i(t) (C_i^h(t) - D_i^h(t)) \\
 &\quad + V_i (C_i^c(t) - E_i^o(t) p^o(t) + C_i^X(t) - R_i^S(t) \\
 &\quad + (G_i^{\text{CHP}}(t) + G_i^b(t)) p^g(t))
 \end{aligned} \quad (56)$$

Since $F_i(t) + V_i p^e(t) < F_i(t) + V_i p^{e,\max} < 0$, IC i tends to increase $E_i(t)$, and $D_i^e(t) = 0$. Thus, $B_i(t+1) \geq B_i(t) \geq 0$.

- 4) Situation 4: $B_i(t) \geq D_i^{e,\max}$. In this situation, $B_i(t+1) = B_i(t) + C_i^e(t) - D_i^e(t) \geq B_i(t) - D_i^e(t) \geq 0$.

Combining the above four situations, Lemma 1 is still valid at time $t+1$, and it is proved. Similarly, the capacity constraint of $W_i(t)$ can be guaranteed. \square

Accordingly, the performance of our proposed method is given

Theorem 1. The time average total cost implemented by our proposed method satisfies:

$$\lim_{T \rightarrow \infty} \frac{1}{T} \sum_{t=0}^{T-1} \mathbb{E}\{C_i(t)\} \leq C_i^{\text{opt}} + \frac{A_i}{V_i}, \forall i \quad (57)$$

where C_i^{opt} denotes the minimum cost of the problem (34).

Proof. $\forall i$, comparing this optimal solution (*) of problem (54) got by minimizing $\Delta_i(t) + V_i \mathbb{E}\{C_i(t)\}$ with the result of the stationary random policy (Π) , $\Delta_i(t) + V_i \mathbb{E}\{C_i(t)\}$ satisfies

$$\begin{aligned}
 &\Delta_i(t) + V_i \mathbb{E}\{C_i(t)\} \\
 &\leq A_i + \mathbb{E}\{F_i(t)(C_i^{e,*}(t) - D_i^{e,*}(t)) + Z_i(t)(C_i^{\text{h},*}(t) \\
 &\quad - D_i^{\text{h},*}(t)) + V_i(C_i^{c,*}(t) + E_i^*(t)p^e(t) - E_i^{o,*}(t)p^o(t) \\
 &\quad + C_i^{X,*}(t) - R_i^{S,*}(t) + (G_i^{\text{CHP},*}(t) + G_i^{b,*}(t))p^g(t))\} \\
 &\leq A_i + \mathbb{E}\{F_i(t)(C_i^{e,\Pi}(t) - D_i^{e,\Pi}(t)) + Z_i(t)(C_i^{\text{h},\Pi}(t) \\
 &\quad - D_i^{\text{h},\Pi}(t)) + V_i(C_i^{c,\Pi}(t) + E_i^\Pi(t)p^e(t) - E_i^{o,\Pi}(t)p^o(t) \\
 &\quad + C_i^{X,\Pi}(t) - R_i^{S,\Pi}(t) + (G_i^{\text{CHP},\Pi}(t) + G_i^{b,\Pi}(t))p^g(t))\}
 \end{aligned} \quad (58)$$

Based on (37) and the policy (Π) , $\Delta_i(t) + V_i \mathbb{E}\{C_i(t)\}$ satisfies

$$\Delta_i(t) + V_i \mathbb{E}\{C_i(t)\} \leq A_i + V_i C_{ir}^{\text{opt}} \leq A_i + V_i C_i^{\text{opt}} \quad (59)$$

Summing over $t \in \{0, 1, \dots, T-1\}$, the sum satisfies

$$\mathbb{E}\{Y_i(T-1) - Y_i(0)\} + \sum_{t=0}^{T-1} V_i \mathbb{E}\{C_i(t)\} \leq T A_i + T V_i C_i^{\text{opt}} \quad (60)$$

Dividing both sides by $T V_i$ and taking $T \rightarrow \infty$, the time average cost satisfies

$$\lim_{T \rightarrow \infty} \frac{1}{T} \sum_{t=0}^{T-1} \mathbb{E}\{C_i(t)\} \leq C_i^{\text{opt}} + \frac{A_i}{V_i} \quad (61)$$

\square

According to Lemma 1 and Theorem 1, the cost implemented by our proposed method will arbitrarily approach the optimal cost as the capacities of the energy storage of IC i increase.

IV. SIMULATION RESULT

A. Scene and Setup

This paper considers the carbon and energy trading among four typical ICs in the Hongdou industrial park in Wuxi, Jiangsu Province, China. These four ICs are in turn: a biomedical industry, a plastics industry, an emerging research and development industry and a textile industry. The carbon emission intensities for gas-fired and coal-fired generation are 0.3 tCO₂/MWh and 0.85 tCO₂/MWh, respectively [26]. Other relevant parameters are shown in Table I, which are similar to [33].

To verify the proposed algorithm, the following two methods are introduced. Method 1 is a stochastic gradient-based

TABLE I: Parameters

Parameter	Value	Parameter	Value
B_i^{\max}, W_i^{\max}	4 MWh	p^g	0.4 ¥/KWh
$C_i^{h,\max}, D_i^{h,\max}$	0.4 MWh	η_i^{p2g}	60%
$C_i^{e,\max}, D_i^{e,\max}$	0.4 MWh	l	5 tCO ₂
α, β	1	η_i^{bg}	85%

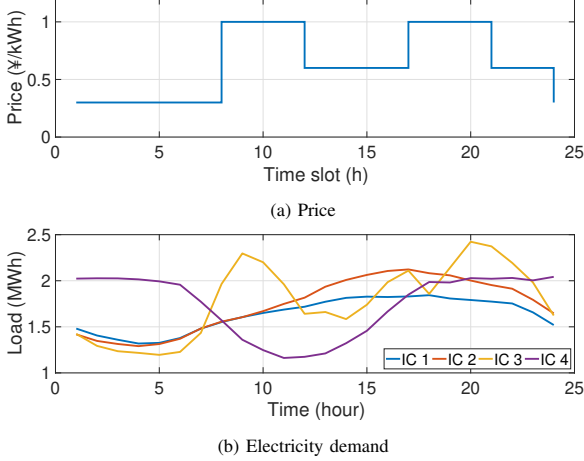


Fig. 5: Data of the industrial park.

algorithm (denoted as SGA) without renewable energy, which is similar to [34]. To evaluate the performance of Lyapunov optimization, Method 2 is adopted, where Lyapunov optimization is replaced by a game-based decision algorithm (denoted as GDA) without queue, similar to [35]. In addition, for fairness, the carbon and energy trading in the baseline methods are similar to our proposed method. The timescales for carbon and energy trading are one day and one hour, respectively. Fig. 5 (a) shows the energy price of JiangSu Electric Power Company [36]. Fig. 5 (b) shows the load of the Hongdou industrial park [37].

B. Results

Coordinating carbon trading and carbon capture (CCTCC) helps high-emitting ICs comply with emission limits. The total costs of the ICs are lower with CCTCC, as shown in Fig. 6. The total costs of ICs consist of energy cost from the CCPP, the gas plant and other ICs, carbon trading cost and green certificate income, where the timescale of carbon trading is set as one day. The calculation results with and without CCTCC for ICs are denoted as Tables II and III. The ICs without CCTCC need to buy electricity from the CCPP with maximum carbon capture power (CCPPMP). Otherwise, they will pay huge fines. The cost of carbon capture is transferred to the ICs, which incurs the prices of CCPPMP to be higher than grid electricity prices. By using the electricity from the CCPPMP, the ICs with additional carbon rights can earn green certificate revenue. For IC i with CCTCC, when the transaction cost exceeds the carbon capture cost, the IC will capture this part of carbon emissions through carbon capture. The remaining carbon emissions are transferred to ICs with lower carbon emissions in the form of carbon trading to achieve a balance between carbon emissions and carbon quotas. The efficiency

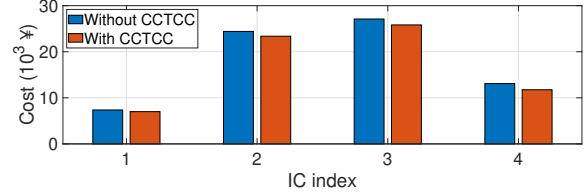


Fig. 6: Total costs of four ICs with and without CCTCC.

TABLE II: Calculation result without CCTCC for ICs in one day

IC	IC1	IC2	IC3	IC4
From the CCPPMP (MWh)	11.42	14.64	16.55	16.58
From the gas plant (MWh)	19.62	26.39	33.75	20.48
Energy cost ($\times 10^3$ ¥)	8.56	25.25	27.83	14.22
Carbon emission (tCO ₂)	7.34	9.78	12.24	8.26
Carbon capture (tCO ₂)	8.25	10.58	11.96	11.98
Carbon quota (tCO ₂)	15.67	16.64	17.10	16.77
Green certificate revenue ($\times 10^3$ ¥)	1.17	0.87	0.49	1.20
Total cost ($\times 10^3$ ¥)	7.39	24.38	27.34	13.02

TABLE III: Calculation result with CCTCC for ICs in one day

IC	IC1	IC2	IC3	IC4
From the CCPP (MWh)	13.41	17.48	18.66	19.47
From the gas plant (MWh)	17.52	24.83	31.89	17.02
Energy cost ($\times 10^3$ ¥)	6.91	22.86	25.32	11.26
Carbon emission (tCO ₂)	16.65	22.31	25.43	21.66
Carbon capture (tCO ₂)	0	0.67	3.33	0
Carbon quota (tCO ₂)	15.67	16.64	17.10	16.77
Carbon trading cost ($\times 10^3$ ¥)	0.10	0.50	0.50	0.49
Total cost ($\times 10^3$ ¥)	7.01	23.36	25.82	11.75

of CCPPMP is 85%, and the carbon trading price $p^c = 100$ ¥/tCO₂.

The cost, electricity trading and battery dynamics for four ICs with and without CCTCC are shown in Fig. 7-9. In trading, a negative value means selling energy, a positive value means purchasing energy. ICs have lower costs under CCTCC in most time slots, as shown in Fig. 7, where ICs with CCTCC can flexibly coordinate the amount of carbon capture and carbon trading based on their cost, whereas ICs without CCTCC may purchase high-priced electricity from CCPPMP or pay huge fines for carbon emissions violations. To reduce the amount of high price electricity purchased from CCPPMP, ICs 2 and 3 without CCTCC purchase more electricity from ICs 1 and 4 to reduce the energy cost, as shown in Fig. 8. For the same reason, ICs without CCTCC charge less electricity into batteries, which also reduces the purchase of the high-priced electricity from CCPPMP, as shown in Fig. 9.

Energy trading helps ICs alleviate energy supply and demand imbalance. Fig. 10 shows that with electricity trading, the cost of the four ICs are reduced. According to Fig. 11, when there is no electricity trading among the ICs, the four ICs trade more gas to make up the energy deficiency. Thus, the cost reduction is not significant.

Fig. 12 shows that the ICs reduce costs through electricity and gas trading, where there is a significant cost reduction for ICs 1 and 4, and a slight cost reduction for ICs 2 and 3. With electricity and gas trading, ICs 1 and 4 can sell electricity and gas to ICs 2 and 3, instead of selling electricity at low prices to the power grid or storing large amounts of energy. Fig. 13 shows that ICs 1 and 4 without energy trading charge more electricity. Thus, the costs of ICs 1 and 4 are greatly reduced. Although ICs 2 and 3 with energy trading can purchase low-

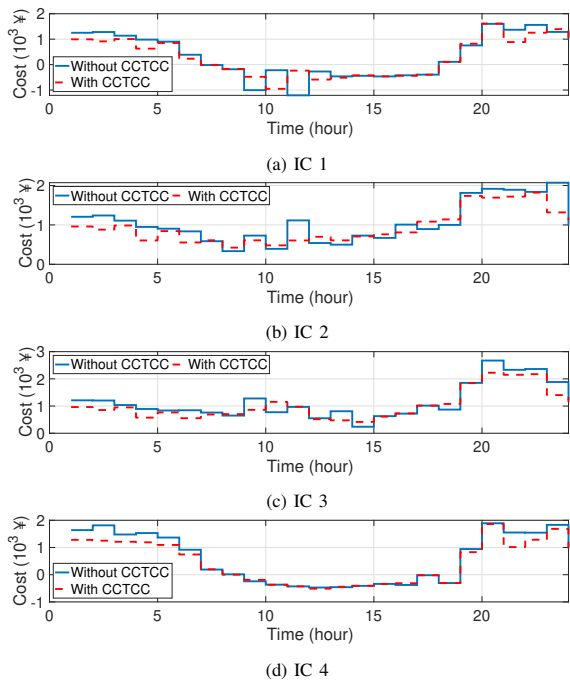


Fig. 7: Cost comparison for four ICs with and without CCTCC.

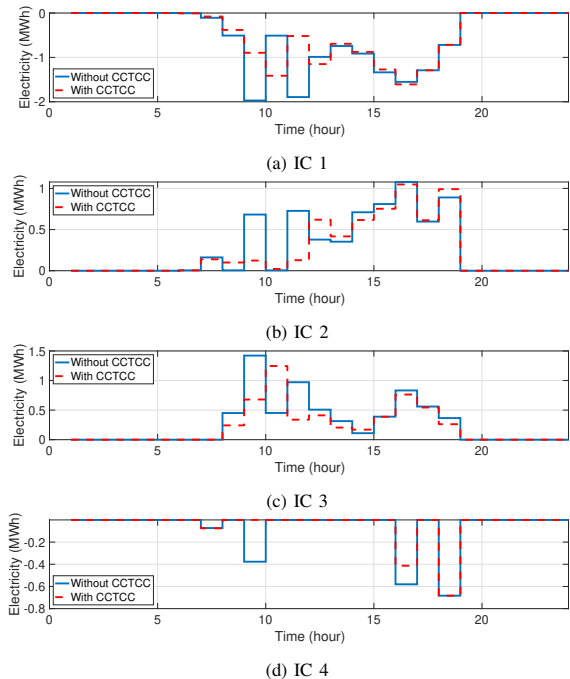


Fig. 8: Electricity trading for four ICs with and without CCTCC.

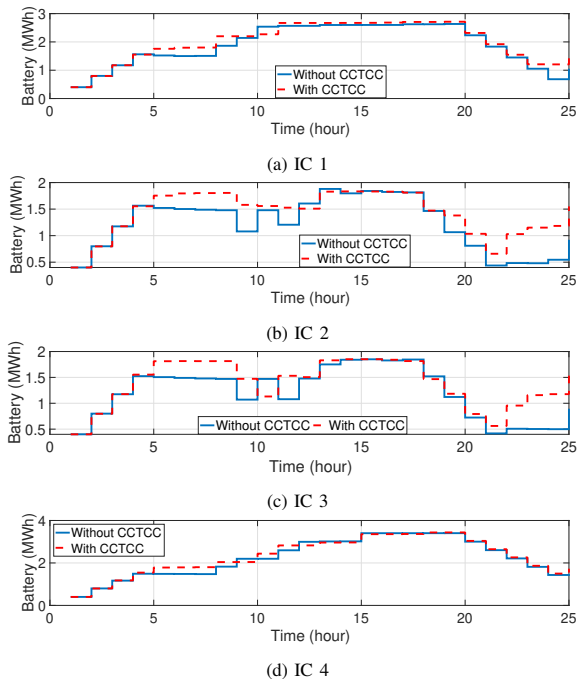


Fig. 9: Battery level for four ICs with and without CCTCC.

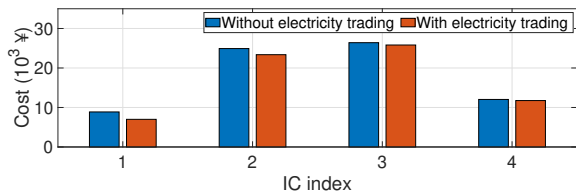


Fig. 10: Total costs of four ICs with and without electricity trading.

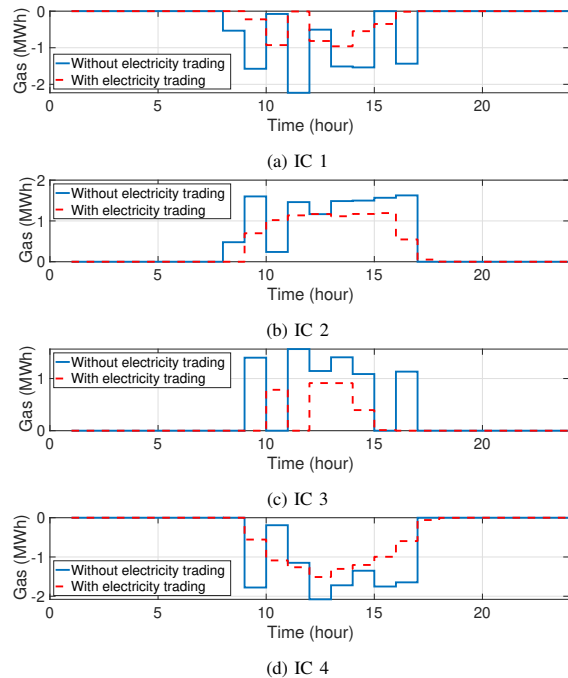


Fig. 11: Gas trading for four ICs with and without electricity trading.

priced energy from ICs 1 and 4, ICs 2 and 3 without energy trading can generate electricity and heat by CHP instead of purchasing high-priced electricity from the power grid. Thus, the cost reduction for ICs 2 and 3 is less. Additionally, Fig. 13 shows that ICs 2 and 3 with energy trading charge more electricity during 12:00-17:00 and discharge electricity to supply the electricity demand during the high-priced periods 17:00-21:00, which reflects the advantages of energy storage.

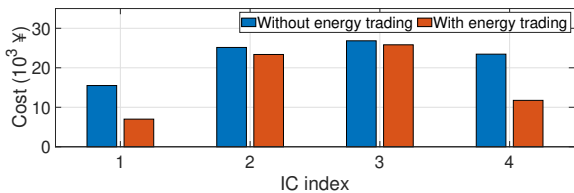


Fig. 12: Total costs of four ICs with and without energy trading.

Since carbon and energy trading are not popularized at present, the total cost comparison of our proposed method with the method lacking CCTCC and energy trading is given in Fig. 14, which demonstrates the effectiveness of the proposed method.

To confirm the performance of Lyapunov optimization, the total costs of four ICs under different energy storage (i.e., battery and water tank) capacities are shown in Fig. 15. The simulation shows that the larger the energy storage capacity, the lower the cost. It agrees with Theorem 1, where the cost gap decreases with V .

Fig. 16 shows the total costs of four ICs under SGA, GDA and the proposed algorithm. Fig. 17 shows the cost comparison for four ICs at 24 hours under SGA, GDA and the proposed algorithm. The overall cost under SGA approaches the overall cost under the proposed algorithm during 0:00-6:00, but more energy needs to be purchased during the day owing to lack

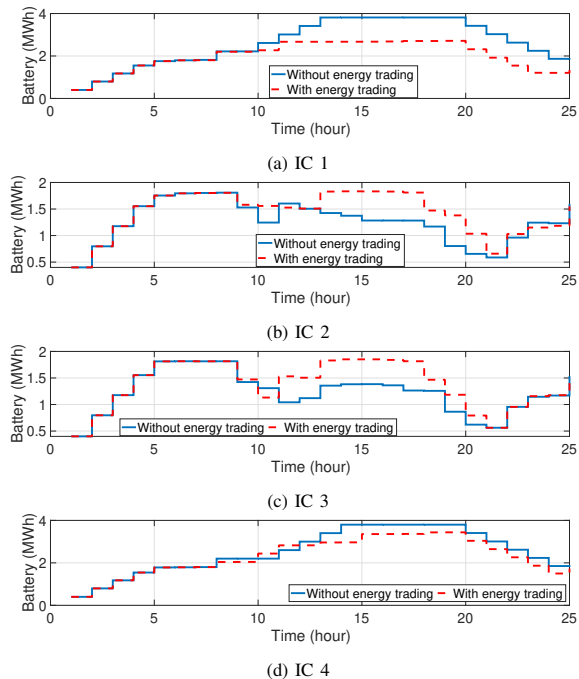


Fig. 13: Battery level for four ICs with and without energy trading.

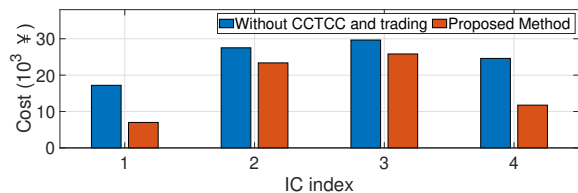


Fig. 14: Total cost comparison of our proposed method with the method lacking CCTCC and energy trading.

of renewable energy, which causes higher cost. Since energy charging and discharging will not directly reduce the energy cost under GDA (i.e., without considering queue backlogs), the ICs cannot make full use of the battery and water tank, resulting in higher cost under GDA. In summary, the proposed algorithm can take full advantage of energy storage, minimize the time-average cost and ensure online energy scheduling.

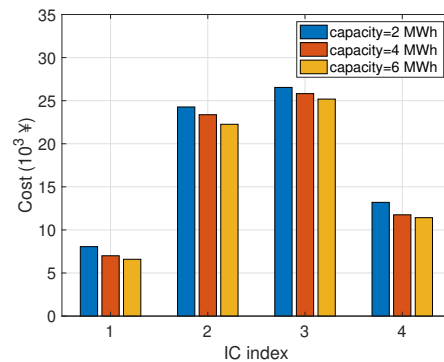


Fig. 15: Total costs of four ICs under different energy storage capacities.

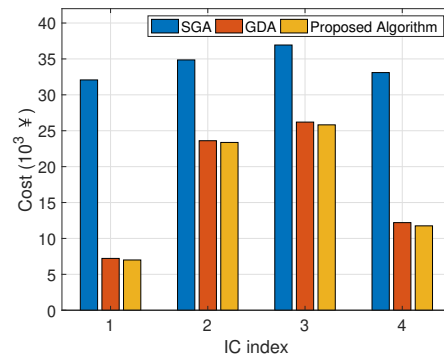


Fig. 16: Total costs of four ICs under different methods.

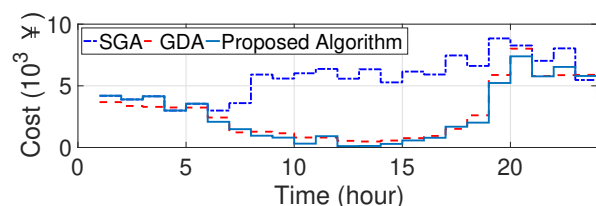


Fig. 17: Cost comparison of four ICs under different methods.

V. CONCLUSION

The carbon emission and energy management problem of industrial clusters is investigated in this paper. A carbon and energy management framework is presented to achieve low-carbon energy scheduling, where a carbon flow model accompanying multi-energy flows is adopted to track and suppress carbon emissions on the user side. A bound tightening algorithm for constraints relaxation is adopted to deal with the quadratic constraint of gas flows. A carbon and energy trading model is constructed. The willingness to trade is improved by the ladder reward and punishment mechanism of carbon trading. A multi-energy trading and scheduling method combining Lyapunov optimization and matching game is presented, which further alleviates the imbalance of supply and demand and maximizes revenue. Finally, simulation results show that each industrial cluster reduces energy costs and carbon emissions, while relieving energy pressure.

In this paper, four industrial clusters are considered in the industrial park. In some scenarios, a park may consist of more clusters. In addition, the energy efficiency and carbon emissions of industrial production can be improved by optimizing the production process. Therefore, joint trading and scheduling among more prosumers needs to be considered, such as [38], to significantly improve the social welfare. In addition, the industrial production process needs to be optimized, like [39], to adapt to the energy and emission requirements.

REFERENCES

- [1] J. Wei, Y. Zhang, J. Wang and L. Wu, "Distribution LMP-Based Demand Management in Industrial Park via a Bi-Level Programming Approach," *IEEE Transactions on Sustainable Energy*, vol. 12, no. 3, pp. 1695-1706, July 2021.
- [2] Q. Liu et al., "Asynchronous Decentralized Federated Learning for Collaborative Fault Diagnosis of PV Stations," *IEEE Transactions on Network Science and Engineering*, vol. 9, no. 3, pp. 1680-1696, 1 May-June 2022.
- [3] M. Gil, P. Dueñas and J. Reneses, "Electricity and Natural Gas Interdependency: Comparison of Two Methodologies for Coupling Large Market Models Within the European Regulatory Framework," *IEEE Transactions on Power Systems*, vol. 31, no. 1, pp. 361-369, Jan. 2016.
- [4] P. Pinson, L. Mitridati, C. Ordoudis and J. Østergaard, "Towards fully renewable energy systems: Experience and trends in Denmark," *CSEE Journal of Power and Energy Systems*, vol. 3, no. 1, pp. 26-35, March 2017.
- [5] M. Paepé, D. Mertens, "Combined heat and power in a liberalised energy market," *Energy Conversion and Management*, vol. 48, no. 9, pp. 2542-2555, Sep. 2007.
- [6] H. Averfalk, P. Ingvarsson, U. Persson, M. Gong and S. Werner, "Large heat pumps in Swedish district heating systems," *Renewable and Sustainable Energy Reviews*, vol. 79, pp. 1275-1284, Nov. 2017.
- [7] G. Papaefthymiou, B. Hasche and C. Nabe, "Potential of Heat Pumps for Demand Side Management and Wind Power Integration in the German Electricity Market," *IEEE Transactions on Sustainable Energy*, vol. 3, no. 4, pp. 636-642, Oct. 2012.
- [8] M. Nielsen, J. Morales, M. Zugno, T. Pedersen and H. Madsen, "Economic valuation of heat pumps and electric boilers in the Danish energy system," *Applied Energy*, vol. 167, pp. 189-200, April 2016.
- [9] Y. Zou, Y. Xu, X. Feng, R. T. Naayagi and B. Soong, "Transactive Energy Systems in Active Distribution Networks: A Comprehensive Review," in *CSEE Journal of Power and Energy Systems*, vol. 8, no. 5, pp. 1302-1317, September 2022.
- [10] S. Chen, Z. Wei, G. Sun and Z. Yizhou, "Strategic Investment in Power and Heat Markets: A Nash-Cournot Equilibrium Model," *IEEE Transactions on Industrial Informatics*, vol. 18, no. 9, pp. 6057-6067, Sept. 2022.
- [11] D. Xu et al., "Peer-to-Peer Multienergy and Communication Resource Trading for Interconnected Microgrids," *IEEE Transactions on Industrial Informatics*, vol. 17, no. 4, pp. 2522-2533, April 2021.
- [12] N. Liu, L. Zhou, C. Wang, X. Yu, and X. Ma, "Heat-electricity Coupled Peak Load Shifting for Multi-energy Industrial Parks: A Stackelberg Game Approach," *IEEE Transactions on Sustainable Energy*, vol. 11, no. 3, pp. 1858-1869, July 2020.
- [13] W. Zhong, K. Xie, Y. Liu, C. Yang and S. Xie, "Auction Mechanisms for Energy Trading in Multi-Energy Systems," *IEEE Transactions on Industrial Informatics*, vol. 14, no. 4, pp. 1511-1521, April 2018.
- [14] F. Zhang, H. Fang and W. Song, "Carbon market maturity analysis with an integrated multi-criteria decision making method: A case study of EU and China," *Journal of Cleaner Production*, vol. 241, pp. 118296, Dec. 2019.
- [15] M. Bradbury, "An anatomy of an IFRIC interpretation," *Accounting in Europe*, vol. 4, no. 2, pp. 109-122, Dec. 2007.
- [16] S. Chen, A. J. Conejo and Z. Wei, "Conjectural-Variations Equilibria in Electricity, Natural-Gas, and Carbon-Emission Markets," *IEEE Transactions on Power Systems*, vol. 36, no. 5, pp. 4161-4171, Sept. 2021.
- [17] W. Huang, N. Zhang, Y. Cheng, J. Yang, Y. Wang and C. Kang, "Multienergy Networks Analytics: Standardized Modeling, Optimization, and Low Carbon Analysis," *Proceedings of the IEEE*, vol. 108, no. 9, pp. 1411-1436, Sept. 2020.
- [18] X. Wei, X. Zhang, Y. Sun and J. Qiu, "Carbon Emission Flow Oriented Tri-Level Planning of Integrated Electricity-Hydrogen-Gas System with Hydrogen Vehicles," *IEEE Transactions on Industry Applications*, vol. 58, no. 2, pp. 2607-2618, April 2022.
- [19] R. Wang, X. Wen, X. Wang, Y. Fu, and Y. Zhang, "Low carbon optimal operation of integrated energy system based on carbon capture technology, LCA carbon emissions and ladder-type carbon trading," *Applied Energy*, vol. 311: 118664, April 2022.
- [20] C. Kang et al., "Carbon Emission Flow From Generation to Demand: A Network-Based Model," *IEEE Transactions on Smart Grid*, vol. 6, no. 5, pp. 2386-2394, Sept. 2015.
- [21] Y. Cheng, N. Zhang, Z. Lu, and C. Kang, "Planning Multiple Energy Systems Toward Low-Carbon Society: A Decentralized Approach," *IEEE Transactions on Smart Grid*, vol. 10, no. 5, pp. 4859-4869, Sept. 2019.
- [22] W. Shen, J. Qiu, K. Meng, X. Chen and Z. Y. Dong, "Low-Carbon Electricity Network Transition Considering Retirement of Aging Coal Generators," *IEEE Transactions on Power Systems*, vol. 35, no. 6, pp. 4193-4205, Nov. 2020.
- [23] Y. Wang, J. Qiu, Y. Tao and J. Zhao, "Carbon-Oriented Operational Planning in Coupled Electricity and Emission Trading Markets," *IEEE Transactions on Power Systems*, vol. 35, no. 4, pp. 3145-3157, July 2020.
- [24] P. Li, W. Sheng, Q. Duan, Z. Li, C. Zhu, and X. Zhang, "A Lyapunov Optimization-Based Energy Management Strategy for Energy Hub With Energy Router," *IEEE Transactions on Smart Grid*, vol. 11, no. 6, pp. 4860-4870, Nov. 2020.
- [25] X. Chen et al., "Increasing the Flexibility of Combined Heat and Power for Wind Power Integration in China: Modeling and Implications," *IEEE Transactions on Power Systems*, vol. 30, no. 4, pp. 1848-1857, July 2015.
- [26] Y. Cheng, N. Zhang, Y. Wang, J. Yang, C. Kang and Q. Xia, "Modeling Carbon Emission Flow in Multiple Energy Systems," *IEEE Transactions on Smart Grid*, vol. 10, no. 4, pp. 3562-3574, July 2019.
- [27] S. Lakshminarayana, T. Q. S. Quek and H. V. Poor, "Cooperation and Storage Tradeoffs in Power Grids With Renewable Energy Resources," *IEEE Journal on Selected Areas in Communications*, vol. 32, no. 7, pp. 1386-1397, July 2014.
- [28] S. Gupta, V. Kekatos and W. Saad, "Optimal Real-Time Coordination of Energy Storage Units As a Voltage-Constrained Game," *IEEE Transactions on Smart Grid*, vol. 10, no. 4, pp. 3883-3894, July 2019.
- [29] G. Leonidas, N. Michael and T. Leandros, "Resource allocation and cross-layer control in wireless networks," *Foundations and Trends in Networking*, vol. 1, no. 1, pp. 1-144, April 2006.
- [30] D. Zhu, B. Yang, Q. Liu, K. Ma, S. Zhu, C. Ma, and X. Guan, "Energy trading in microgrids for synergies among electricity, hydrogen and heat networks," *Applied Energy*, vol. 272: 115225, Aug. 2020.
- [31] S. Chen, A. J. Conejo, R. Sioshansi and Z. Wei, "Unit Commitment With an Enhanced Natural Gas-Flow Model," *IEEE Transactions on Power Systems*, vol. 34, no. 5, pp. 3729-3738, Sept. 2019.
- [32] JW. Hatfield and SD. Kominers, "Contract design and stability in many-to-many matching," *Games and Economic Behavior*, vol. 101, pp. 78-97, Jan. 2017.
- [33] D. Zhu, B. Yang, C. Ma, Z. Wang, S. Zhu, K. Ma and X. Guan, "Stochastic gradient-based fast distributed multi-energy management for an industrial park with temporally-coupled constraints," *Applied Energy*, vol. 317: 119107, July 2022.

- [34] R. Deng, Z. Yang, J. Chen and M. -Y. Chow, "Load Scheduling With Price Uncertainty and Temporally-Coupled Constraints in Smart Grids," *IEEE Transactions on Power Systems*, vol. 29, no. 6, pp. 2823-2834, Nov. 2014.
- [35] Y. Wang, W. Saad, Z. Han, H. V. Poor and T. Başar, "A Game-Theoretic Approach to Energy Trading in the Smart Grid," *IEEE Transactions on Smart Grid*, vol. 5, no. 3, pp. 1439-1450, May 2014.
- [36] The price provided by the State Grid Jiangsu Electric Power Co., Ltd, <http://www.js.sgcc.com.cn/html>.
- [37] Z. Wang, B. Yang, W. Wei, S. Zhu, X. Guan and D. Sun, "Multi-Energy Microgrids: Designing, operation under new business models, and engineering practices in China," *IEEE Electrification Magazine*, vol. 9, no. 3, pp. 75-82, Sept. 2021.
- [38] M. H. Ullah and J. -D. Park, "A Two-Tier Distributed Market Clearing Scheme for Peer-to-Peer Energy Sharing in Smart Grid," *IEEE Transactions on Industrial Informatics*, vol. 18, no. 1, pp. 66-76, Jan. 2022.
- [39] R. Li and V. Mahalec, "Integrated design and operation of energy systems for residential buildings, commercial buildings, and light industries," *Applied Energy*, vol. 305: 117822, Jan. 2022.